Stem Cell Reports
Article

ISSCR

OPEN ACCESS

Neural-Competent Cells of Adult Human Dermis Belong to the Schwann Lineage

Usue Etxaniz,[1,8] Adrián Pérez-San Vicente,[1,8] Nuria Gago-López,[1,2,8] Mario García-Dominguez,[3] Haizea Iribar,[1] Ariane Aduriz,[4] Virginia Pérez-López,[1] Izaskun Burgoa,[1] Haritz Irizar,[5] Maider Muñoz-Culla,[5] Ainara Vallejo-Illarramendi,[5] Olatz Leis,[6] Ander Matheu,[7] Angel G. Martín,[6] David Otaegui,[5] María Paz López-Mato,[4] Araika Gutiérrez-Rivera,[1] Robb MacLellan,[2] and Ander Izeta[1,*]

[1]Tissue Engineering Laboratory, Bioengineering Area, Instituto Biodonostia, Hospital Universitario Donostia, Paseo Dr. Begiristain s/n, 20014 San Sebastián, Spain
[2]Division of Cardiology, University of Washington Medical Center, 850 Republican Street, Seattle, WA 98195, USA
[3]Cell Differentiation Lab, Stem Cells Department, Centro Andaluz de Biología Molecular y Medicina Regenerativa (CABIMER), Avenida Americo Vespucio s/n, 41092 Sevilla, Spain
[4]Cell Cytometry and Microscopy Unit, Fundación Inbiomed, Paseo Mikeletegi 81, 20009 San Sebastián, Spain
[5]Neuroscience Area, Instituto Biodonostia, Hospital Universitario Donostia, Paseo Doctor Begiristain s/n, 20014 San Sebastián, Spain
[6]StemTek Therapeutics SL, Rodriguez Arias 23, 48011 Bilbao, Spain
[7]Oncology Area, Instituto Biodonostia, Hospital Universitario Donostia, Paseo Doctor Begiristain s/n, 20014 San Sebastián, Spain
[8]Co-first author
*Correspondence: ander.izeta@biodonostia.org
http://dx.doi.org/10.1016/j.stemcr.2014.09.009

SUMMARY

Resident neural precursor cells (NPCs) have been reported for a number of adult tissues. Understanding their physiological function or, alternatively, their activation after tissue damage or in vitro manipulation remains an unsolved issue. Here, we investigated the source of human dermal NPCs in adult tissue. By following an unbiased, comprehensive approach employing cell-surface marker screening, cell separation, transcriptomic characterization, and in vivo fate analyses, we found that p75NTR$^+$ precursors of human foreskin can be ascribed to the Schwann (CD56$^+$) and perivascular (CD56$^-$) cell lineages. Moreover, neural differentiation potential was restricted to the p75NTR$^+$CD56$^+$ Schwann cells and mediated by *SOX2* expression levels. Double-positive NPCs were similarly obtained from human cardiospheres, indicating that this phenomenon might be widespread.

INTRODUCTION

The search for adult neural precursor cells (NPCs) outside of the CNS has been the focus of extensive research due to the accessibility and envisioned use of these cells in the treatment of neurodegenerative disease. Tissue-specific multipotent cells with the capacity to generate neural (i.e., neuronal and glial) progeny have now been isolated from a number of adult tissues, including bone marrow, fat, heart, intestine, palate, pancreas, skeletal muscle, skin, and uterus. Somewhat less surprisingly, NPCs can also be derived from peripheral nerves, ganglia, enteric glia, and the carotid body. However, even though NPCs can be obtained from diverse tissues, in most instances their origin remains unknown (Joseph and Morrison, 2005).

Among the above-mentioned examples, the skin is arguably the tissue that is the most easily accessible and requires less invasive extraction procedures. Sphere-forming neural-crest-derived adult precursors reside in the dermis (Toma et al., 2001; Wong et al., 2006), and subpopulations of these appear to present stem cell properties (Biernaskie et al., 2009). Using antibodies against the low-affinity neurotrophin receptor p75NTR, previous studies isolated postmigratory neural crest stem cells (NCSCs) from both embryonic and adult tissues (Kruger et al., 2002; Morrison et al., 1999). In this report, we explore the source of NPCs in adult human dermis and find that they originate from p75NTR$^+$CD56$^+$ cells belonging to the Schwann lineage. Further, the expression levels of *SOX* genes seem to be tightly regulated in p75NTR$^+$ cells of human skin, and we show that *SOX2* expression levels correlate with the neural competence of dermal precursors, as described for other systems (Hutton and Pevny, 2011; Kim et al., 2003; Taranova et al., 2006).

RESULTS

We investigated the identity of human NPCs extracted from the foreskin dermis through fluorescence-activated cell sorting (FACS)-based isolation of cell subpopulations and subsequent characterization of the sorted cells (Figure 1). Immunofluorescent and flow-cytometry analyses of sphere cultures showed the existence of a rare p75NTR (also known as Gp80-LNGFR, CD271, and TNFRSF16)-positive cell subpopulation (2.9% ± 1.7% of total; n = 24) in primary dermal sphere cultures that was Nestin$^+$ and CD34$^-$ and presented a characteristic morphology (i.e., a single

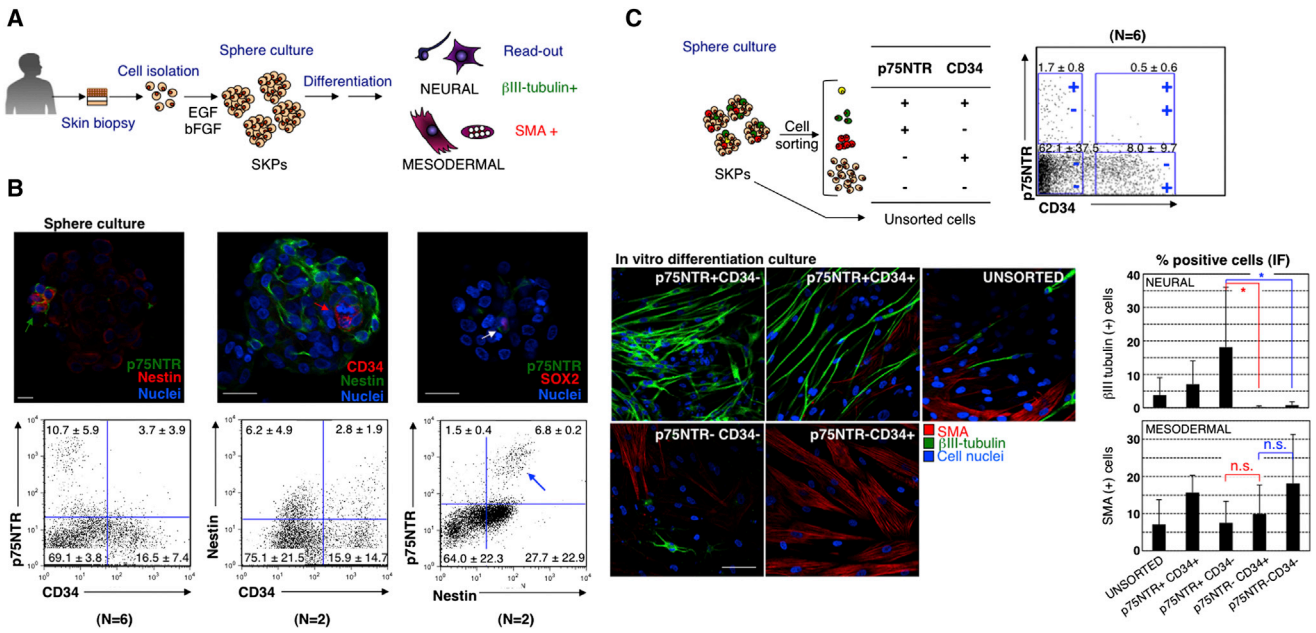

Figure 1. Human Dermospheres Contain p75NTR$^+$ Nestin$^+$ SOX2$^+$ NPCs

(A) Cell isolation and characterization procedure.

(B) Characterization of primary dermospheres by immunofluorescence and confocal microscopy. A subgroup of cells (green arrow) expressed p75NTR and Nestin. In contrast, CD34$^+$ cells (red arrow) were Nestin$^-$. SOX2 colocalized with p75NTR$^+$ cells (white arrow). Nuclei were counterstained with Hoechst 33258 (blue). Scale bars, 10 μm. Flow-cytometry analyses confirmed separate cell subpopulations that were positive for p75NTR and CD34, and a distinct p75NTR$^+$Nestin$^+$ population (blue arrow).

(C) Primary dermospheres were dissociated, double sorted with anti-p75NTR and anti-CD34 antibodies, and put into differentiation culture. Representative stainings for neural (βIII tubulin, green) and mesodermal (SMA, red) progeny are shown. Nuclei were counterstained with Hoechst 33258 (blue). Scale bar, 10 μm. Quantifications of the percentages of neural (upper panel) and mesodermal (lower panel) cells are shown in relation to the total cell number. Statistical significance (one-way ANOVA) values were p = 0.034 (*, n = 6) for the comparison of p75NTR$^+$CD34$^-$ versus p75NTR-CD34$^+$ (neural), p = 0.039 (*, n = 6) for p75NTR$^+$CD34$^-$ versus p75NTR-CD34$^-$ (neural), p = 0.147 (n.s., n = 6) for the comparison p75NTR$^+$CD34$^-$ versus p75NTR-CD34$^+$ (mesodermal), and p = 0.674 (n.s., n = 6) for p75NTR$^+$CD34$^-$ versus p75NTR$^-$ CD34$^-$ (mesodermal). Error bars indicate SD.

See also Table S2 and Movies S1 and S2.

process extending from the soma; Figure 1B; Movie S1 available online). Intriguingly, 74.6% ± 2.9% of p75NTR$^+$ cells coexpressed SOX2 by immunofluorescence analyses (Movie S2), indicating that p75NTR$^+$ cells might be more precursor-like. Isolation of p75NTR$^+$CD34$^-$ cells enabled a significant enrichment of precursors committed to the neural lineage in vitro, as assessed by an average 22.7-fold increase (18.2% versus 0.8% of total cells; n = 6) in their neural differentiation capacity when compared with p75NTR-CD34$^-$ cells (Figure 1C).

To determine whether p75NTR$^+$ cells exhibit the same differentiation potential in ovo, we sorted, expanded, and injected human cells into the neural crest migratory stream (Hamburger-Hamilton stage 17 [HH17] chicken embryos, hindlimb-level somites; Figure 2A). Cross-sections of HH26 embryos, immunolabeled with anti-human nuclei (anti-HuNu) for the detection of transplanted cells, showed that the human p75NTR$^+$ cells survived; migrated to the neural crest, dorsal root ganglia (DRG), and skin; and differentiated into βIII tubulin$^+$ cells (Figures 2B–2F). Since βIII tubulin was recently reported to mark human melanocyte lineage cells, as well as peripheral neurons in the dermis (Locher et al., 2013), we confirmed the peripheral neuronal phenotype of HuNu$^+$ cells by showing coexpression of neurofilament 200 (NF200; Figures 2G–2I). These markers were not present in the original dermal cultures (Figure S1). In contrast, p75NTR$^-$ cells were hardly detected at the HH26 stage, if at all, and most of the surviving cells did not express any of the aforementioned markers (Figures 2J and 2K; data not shown). A quantification of transplant-derived HuNu$^+$ cells showed that, as expected, p75NTR$^+$ NPCs showed increased survival, migration to peripheral tissue, and neural differentiation when compared with both unsorted and p75NTR$^-$ cell fractions. On average, 10.8-fold more p75NTR$^+$ cells survived, migrated to peripheral tissue, and differentiated into peripheral neurons than p75NTR$^-$

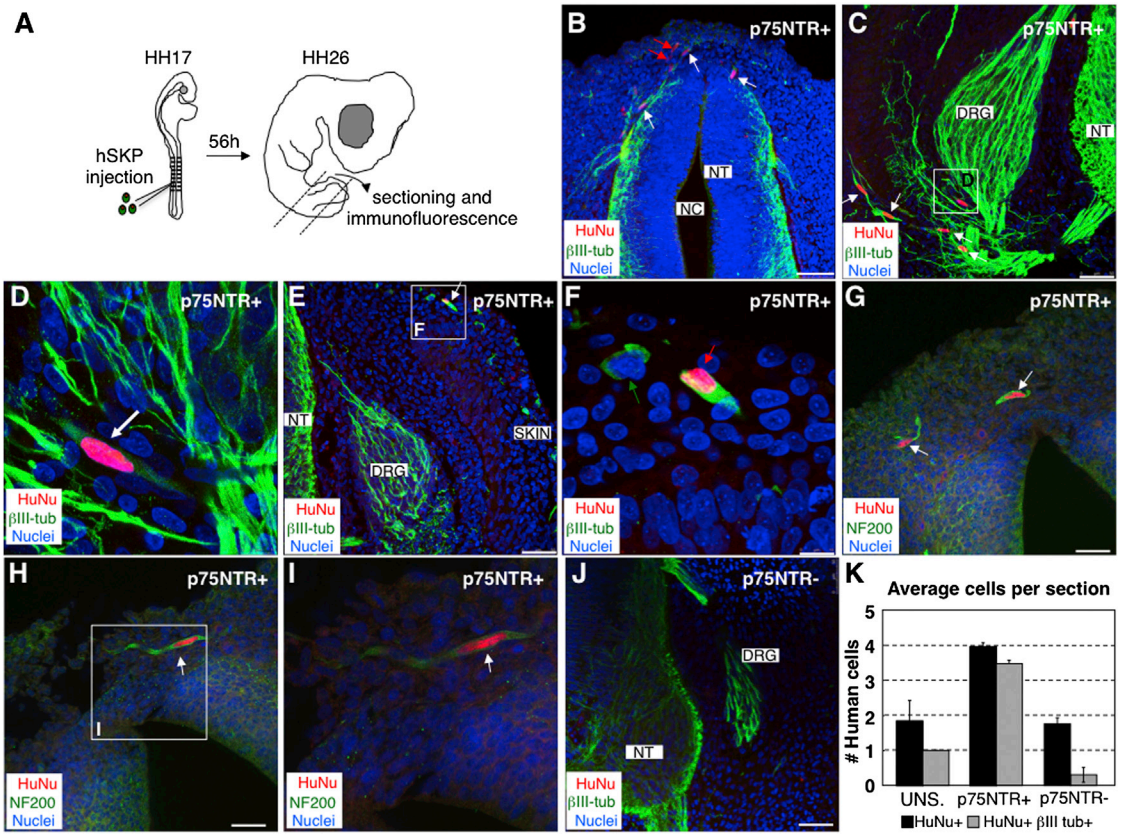

Figure 2. In Ovo Fate of Human Dermis-Derived NPCs

(A) Human cells (p75NTR$^+$, n = 11 embryos; p75NTR$^-$, n = 7; unsorted, n = 7) were injected into somites of HH17 chicken embryos, incubated until the HH26 stage, sectioned, and analyzed by immunofluorescence.

(B–F) Cross-sections of p75NTR$^+$ transplant immunolabeled with anti-human nuclei (HuNu) and anti-βIII tubulin antibodies. NT, neural tube; NC, neural canal; DRG, dorsal root ganglia.

(G–I) Cross-sections of p75NTR$^+$ transplants immunolabeled with anti-HuNu and anti-NF200 antibodies.

(J) In the cross-sections of p75NTR$^-$ cell transplants, HuNu$^+$βIII tubulin$^+$ cells were hardly detected at the HH26 stage, if at all.

(K) Quantification of the average human cell transplant-derived (HuNu$^+$ cells) and HuNu$^+$βIII tubulin$^+$ cells detected per tissue section (unsorted [UNS], n = 2 embryos; p75NTR$^+$, n = 3; p75NTR$^-$, n = 2). In all sections, nuclei were counterstained with Hoechst 33258 (blue). Error bars indicate SD.

See also Figure S1 and Table S2.

cells (Figure 2K). These results confirmed the neurogenic fate of dermis-derived p75NTR$^+$ cells in vivo.

Source of the Human p75NTR$^+$ Dermal Precursors

As the p75NTR is expressed by a number of skin-resident cell types (Adly et al., 2009), we next sought to determine the source of human-skin-derived NPCs by analyzing proteins coexpressed by these cells. Using an unbiased, cell-cytometry-based screen of 242 surface markers, we found that the p75NTR$^+$ cell fraction coexpressed 30 proteins in freshly dissociated (uncultured) cells (Figure 3A). These markers were then validated in dermal sphere cultures, where precursor cells are enriched (Figure 3B). Three cell-surface proteins were specifically upregulated in sphere-forming p75NTR$^+$ cells as compared with the negative fraction, namely, integrin alpha-6 (also known as CD49f), CD56 (also known as PSA-NCAM), and NCAM-L1 (also known as CD171 and L1CAM). These three markers are characteristic of nerve terminal cells, i.e., cells at the peripheral nerve endings innervating the human papillary dermis (Reinisch and Tschachler, 2012). For this reason, we pursued further purification of the neural-competent cells and freshly isolated four cell fractions by using anti-p75NTR and anti-CD56 antibodies. In vitro differentiation analyses unambiguously showed that p75NTR$^+$CD56$^+$ cells (2.85% ± 0.31% of total; n = 7 biopsies analyzed in three independent experiments) were responsible for all dermis-derived neurogenic activity, as shown by an average

103.8-fold increase (25.9% versus 0.2% of total cells) in βIII tubulin$^+$ cell yield when compared with double-negative cells (Figure 3C). In contrast, p75NTR$^+$CD56$^-$ cells had no relevant neural differentiation capacity in vitro. These data demonstrate a neurogenic subpopulation within dermis-derived precursors and thus have profound implications for the use of dermis-derived precursors for neuroregenerative purposes (Hunt et al., 2009).

Adult human dermis-derived precursor cells do not always maintain their biological properties, as they may become senescent when expanded in vitro (Gago et al., 2009; Hill et al., 2012; Liu et al., 2011; Wang et al., 2014). For this reason, we checked in vitro expansion of double-positive p75NTR$^+$CD56$^+$ cells, the most significant dermal precursor subtype for potential clinical use, and relevant numbers of cells that maintained precursor properties were achieved in diverse culture conditions (Figure S2 and data not shown).

We then pursued in situ localization of p75NTR$^+$CD56$^+$ cells in human dermis. When we visualized the cutaneous nerve plexus through whole-mount immunostaining (Figures 4A and 4B; Tschachler et al., 2004), we observed not only Schwann cells stained by anti-p75NTR antibody but also cells with a perivascular localization (Figures 4C–4E; Movie S3). Of note, the latter were not costained by CD56, which enabled us to easily separate the two p75NTR$^+$ cell subpopulations (Schwann and perivascular; Figures 4B–4E; Movie S4). Perivascular p75NTR$^+$ cells coexpressed the markers chondroitin sulfate proteoglycan 4 (CSPG4, also known as NG2; Figures 4F–4H) and α-smooth muscle actin (SMA; Figures 4I–4L), which are characteristic of perivascular cell types (Wanjare et al., 2014). Peripheral-nerve-localized p75NTR$^+$ cells were shown to ensheath ubiquitin carboxyl-terminal esterase L1 (PGP9.5)-positive nerve fibers (Figures 4M–4P), which could also be detected through expression of microtubule-associated protein 2 (MAP2; Figures 4Q–4T) and Peripherin (Figures 4U–4X). These data suggest that neural-competent cells derived from human dermis arise (at least in part) from peripheral-nerve-ensheathing p75NTR$^+$CD56$^+$ Schwann cells.

Dermis-Derived NPCs Belong to the Schwann Cell Lineage

To further identify human skin-derived p75NTR$^+$ cells, we performed a transcriptomic characterization of cell subpopulations sorted directly after skin disaggregation by real-time quantitative RT-PCR (qRT-PCR) (Figure 5A; Table S1). The purity of the cellular fractions was validated through analysis of mRNA expression for the genes *NGFR* (coding for p75NTR), *NCAM1* (CD56), and *MCAM* (CD146). Proteins that were previously identified by immunofluorescence and flow cytometry as positive (integrin α6, NCAM-L1, Nestin, and SOX2) or negative (CD34) in p75NTR$^+$ cells showed correlated expression of the corresponding mRNAs (*ITGA6*, *L1CAM*, *NES*, *SOX2*, and *CD34*, respectively; Figure 5B), thus providing further validation of the gene-expression data. The expression levels of the 95 mRNAs that were analyzed efficiently discriminated three dermal cell subpopulations: p75NTR$^+$CD56$^+$ (Schwann), p75NTR$^+$CD56$^-$ (perivascular), and p75NTR-CD56$^-$ (non-Schwann, nonperivascular) (Figures 5C and 5D).

We first analyzed the expression of markers of the Schwann cell lineage (Figure S3; Jessen and Mirsky, 2005) in the three dermis-derived cell subpopulations. Genes shared by embryonic NCSCs and Schwann cell precursors (SCPs), such as *CDH2*; SCP-specific (*CDH19*), as well as genes shared by SCPs and immature Schwann cells (iSCs, such as *PMP22*, *PLP1*, and *DHH*) were found to be upregulated in p75NTR$^+$CD56$^+$ cells (Figure 5E), further demonstrating their Schwann cell lineage identity.

As anticipated from their perivascular localization and cell-surface marker profile, the p75NTR$^+$CD56$^-$ cells upregulated a robust number of marker pericyte genes (Armulik et al., 2011; Paquet-Fifield et al., 2009) when compared with the p75NTR$^+$CD56$^+$ cells (Figure 5F). Somewhat unexpectedly, perivascular (p75NTR$^+$CD56$^-$) cells also upregulated most of the Schwann lineage genes as compared with p75NTR$^-$ cells, although at generally lower levels than p75NTR$^+$CD56$^+$ cells.

To explore the relationship between dermal p75NTR$^+$ cells and skin-derived precursors (SKPs), we analyzed known markers for the latter (Fernandes et al., 2004; Toma et al., 2001, 2005). SKP genes were overexpressed by the p75NTR$^-$ fraction (Figure 5G), indicating that SOX2$^+$ cells either arise from a lineage distinct from that of SKPs or are detected at a different stage (Johnston et al., 2013). Although p75NTR$^+$ cells do not express markers of the dermal papilla niche (contrary to their murine hair follicle counterparts, which overexpress *VCAN*, *WNT5A*, *BMP4*, *ALPL*, and *SERPINE2*; Figure S4A), recent evidence indicates that murine SOX2$^+$ follicle-associated precursor cells may also be derived from peripheral nerves (Johnston et al., 2013). In fact, an analysis of published microarray data (Biernaskie et al., 2009; Driskell et al., 2009) shows that *NGFR*, *ERBB3*, *MPZ*, *PLP1*, and *S100B* are significantly upregulated in SOX2$^+$ follicle-associated dermal stem cell fractions (Figures S4B and S4C). Moreover, they significantly upregulate expression of *CDH2*, a marker of terminal Schwann cells of the hair follicle bulb (Kaidoh and Inoué, 2008). These results indicate that SOX2$^+$ cells derived from mouse hair follicle and human nonhairy skin may be phenotypically equivalent, with expression of dermal papilla (niche) markers being a major difference between them.

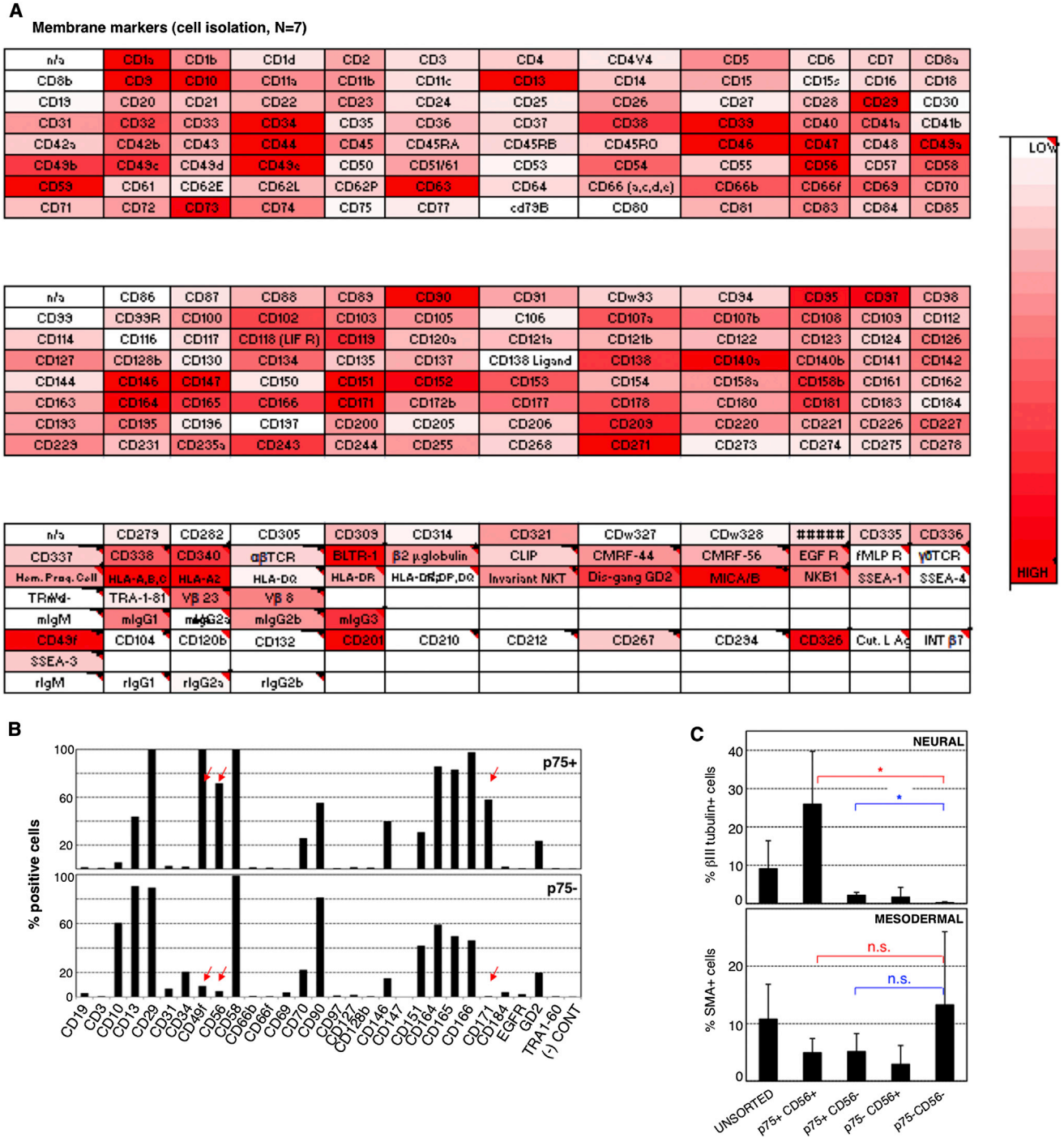

Figure 3. Human Dermis-Derived NPCs Express Markers Characteristic of the Schwann Lineage

(A) The expression of p75NTR and coexpression of 242 membrane markers were analyzed by flow cytometry of freshly disaggregated biopsies (n = 7).

(B) Markers that were high in the p75NTR$^+$ fraction, but not in the negative cells, were validated in dermal sphere cultures (n = 6). As controls, markers that were highly expressed (CD29 and CD58) and negative (CD3 and CD19) in both fractions were included.

(C) In vitro differentiation of freshly sorted cell fractions and quantification of neural (βIII tubulin$^+$) and mesodermal (SMA$^+$) progeny. Quantifications of the percentages of neural (upper panel) and mesodermal (lower panel) cells are shown in relation to the total cell

(legend continued on next page)

SOX2 Regulates Neural Competence of Dermal Precursor Cells

As detected by qRT-PCR, *SOX2* and *SOX10* expression levels were approximately 40% lower in perivascular cells than in Schwann cells (Figure 5E), i.e., their gene-expression levels correlated with a loss of neural competence in other stem cell systems (Wegner, 2011). In accord with this, SOX2-regulated genes such as *CDH2*, *NOTCH1*, *PAX3*, and *PLP1* (Bergsland et al., 2011) were also transcribed to a lower extent in perivascular cells. On the other hand, *SOX9* was strongly and specifically downregulated in p75NTR$^+$CD56$^+$ cells (Figure 5G). Since Schwann and perivascular cells share an important number of markers, we posit a model of three alternative states of dermis-derived precursor cells, the regulation of which might be mediated by *SOX* gene-expression levels (Figure 6A). Although the three precursor cell states generate mesodermal progeny, only p75NTR$^+$CD56$^+$ (i.e., *SOX2*^{hi}) cells retain neural competence. Indirect support for this idea comes from the adult mouse pituitary gland, where sphere-forming resident stem cells become SOX2$^+$SOX9$^-$, and differentiated cells become Nestin$^+$, SOX9$^+$, and S100β$^+$ (Fauquier et al., 2008).

To test this model, we used *SOX2*^{EGFP} mice (Ellis et al., 2004). Dermis-derived and subventricular zone (SVZ)-derived cells were separated into SOX2 negative, low, medium, and high subpopulations according to their EGFP expression levels by FACS (Figures 6B and 6C). Dermis-derived cells were separated into four fractions, in which EGFP expression levels correlated with endogenous SOX2 (by flow cytometry; Figure 6D) and also with *SOX2* mRNA levels (by qRT-PCR; Figure 6E). In contrast, most SVZ-derived cells (97.7% in n = 5 pooled biopsies) were found in the EGFP^{med} fraction. Interestingly, the neural competence of the murine dermal cell subpopulations correlated with *SOX2*^{EGFP} levels, as expected, with the EGFP^{hi} fraction reaching similar differentiation levels compared with unsorted SVZ cultures (as determined by percent βIII tubulin$^+$ cells; Figure 6F). To validate these murine results in human cultures, we performed gain- and loss-of-function experiments by using lentiviral constructs to constitutively augment and silence *SOX2* expression (Figure 6G). Stable overexpression of SOX2-mCitrine in p75NTR$^+$CD56$^-$ cells resulted in neural competence that correlated with mCitrine levels (Figure 6H). In the opposite direction, p75NTR$^+$CD56$^+$ NPCs that were transduced with *SOX2*-specific shRNA lentivirus reduced *SOX2* mRNA expression levels and abolished neural differentiation capacity as compared with cells transduced with the empty vector (Figure 6I).

Finally, and taking into account that human foreskin-derived SKPs can make myelinating Schwann cells (Krause et al., 2014), we pursued in vitro derivation of myelin-producing Schwann cells in order to test the relevance of *SOX2* expression levels in this context (Figure S5). When they were predifferentiated to Schwann cells for 4 days, human dermis-derived p75NTR$^+$CD56$^+$ cells expressed galactocerebroside (GalC; Figures S5A–S5D), but not myelin basic protein (MBP; Figures S5E–S5H), as expected (Lemke and Chao, 1988; Ranscht et al., 1982). Spinal cord and DRG explants from embryonic day 14 (E14) rats were then prepared and added to predifferentiated Schwann cultures (Biernaskie et al., 2009; Chen et al., 2010). Under these conditions, human dermis-derived p75NTR$^+$CD56$^+$ cells, visualized by both anti-HuNu and anti-GFP staining (after constitutive transduction with an EGFP-expressing lentiviral construct), became MBP$^+$ and myelinated axons in vitro (Figures S5I–S5P). Further, their ability to myelinate axons was dramatically reduced when the cells were previously transduced with *SOX2*-specific shRNA lentivirus (Figure S5Q). Overall, these results demonstrated the pivotal role of *SOX2* in regulating the neural competence of dermis-derived precursors.

p75NTR$^+$CD56$^+$ NPCs May Also Be Derived from Human Heart

Since NPCs are related to the peripheral nerves, the data obtained for dermis precursors may be pertinent to NPCs derived from multiple organs. To give some experimental support to this speculation, we sorted human heart-derived precursors by FACS with anti-p75NTR and anti-CD56 antibodies (Figure 7A). In vitro differentiated p75NTR$^+$CD56$^+$ cells displayed an average 13.8-fold increase (20.8% versus 1.5% of total cells, n = 2) in βIII tubulin$^+$ cell formation when compared with double-negative heart cells (Figure 7B). In agreement with the skin results, heart-derived p75NTR$^+$CD56$^-$ cells showed no relevant neural differentiation capacity in vitro.

DISCUSSION

This study provides experimental evidence that primary dermospheres obtained from human skin contain a mixture of SOX2$^+$ multipotent precursors and more committed cells, with SOX2$^+$ cells being derived from either Schwann or perivascular cells. It also suggests that *SOX2* expression levels are tightly regulated in dermal precursors and

number. Statistical significance (one-way ANOVA) values were p = 0.032 (*, n = 3) for the comparison p75NTR$^+$CD56$^+$ versus p75NTR-CD56$^-$ (neural), p = 0.014 (*, n = 3) for p75NTR$^+$CD56$^-$ versus p75NTR-CD56$^-$ (neural), p = 0.345 (n.s., n = 3) for p75NTR$^+$CD56$^+$ versus p75NTR-CD56$^-$ (mesodermal), and p = 0.360 (n.s., n = 3) for p75NTR$^+$CD56$^-$ versus p75NTR-CD56$^-$ (mesodermal). Error bars indicate SD.
See also Figure S2.

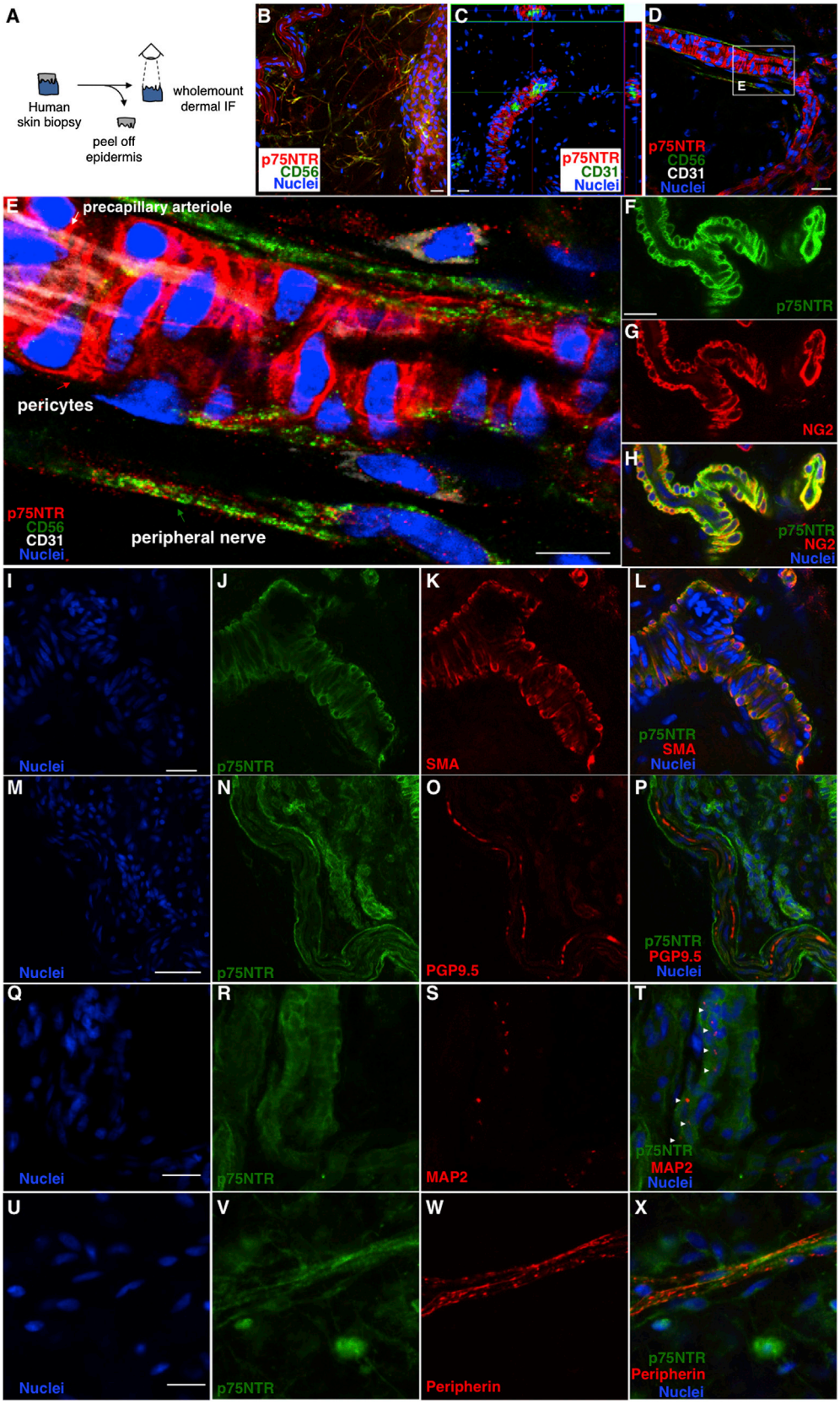

(legend on next page)

determine the ability of these cells to generate neural progeny. Embryonic Schwann cell markers such as *CDH2* and *CDH19* are known to be sharply downregulated in Schwann embryonic development at the iSC stage (Takahashi and Osumi, 2005; Wanner et al., 2006), and thus upregulation of these mRNAs in adult Schwann cells is unexpected (Mirsky et al., 2002). It is tempting to speculate that their appearance in the double-positive cells suggests a resident precursor cell status; alternatively, it may reflect Schwann cell dedifferentiation as a result of dermal disaggregation procedures (Jessen and Mirsky, 2008; Parrinello et al., 2010). Of note, recent murine data demonstrated that cellular dedifferentiation plays a major part in *SOX2* upregulation in these cells (Johnston et al., 2013). The extent to which cellular dedifferentiation is related to the appearance of human dermis-derived NPCs in sphere culture and beyond remains to be determined.

Our data hint at a previously unrecognized relationship between postnatal foreskin-derived Schwann and perivascular cells, as deduced from their strikingly similar gene-expression profiles. Alternatively, the two cell subtypes might reflect a single, highly dynamic cell precursor with environmental differences playing a role in distinctive cellular states (Biernaskie et al., 2009). This will remain an open question until lineage-tracing experiments can unambiguously show the developmental relationship (if any) between Schwann and perivascular cells. In any case, our data support the notion that specialized Schwann cells at the peripheral nerve endings in the skin retain the capacity to dedifferentiate to the NPC stage, as recently hypothesized (Dupin and Sommer, 2012; Kaucká and Adameyko, 2014). Of note, human cerebral cortex pericytes have been reprogrammed into induced neuronal cells by overexpression of *SOX2* and *MASH1* (Karow et al., 2012), and glioma stem cells give rise to pericytes (in support of tumor growth) while downregulating *SOX2* expression (Cheng et al., 2013).

In summary, we have presented a simple method to isolate NPCs from human skin through cell sorting. Further, we have demonstrated that cardiosphere-derived p75NTR$^+$CD56$^+$ cells also constitute NPCs. Intriguingly, nerve-terminal-associated SOX2$^+$ neural crest precursors ("NT cells") are also found in mouse skin and have been reported to have a potential role in wound repair (Johnston et al., 2013). Further, murine NT cells share a number of markers with human p75NTR$^+$CD56$^+$ cells and induce *SOX2* expression upon injury. Our own data suggest that mouse NT cells might be dermal NPCs, as is the case in humans, and the regulation of potency mediated by *SOX2* levels might explain the observed derivation of Schwann cells out of mesodermal lineages (Jinno et al., 2010; Krause et al., 2014). This particular point awaits experimental confirmation. Although no evidence implicating human p75NTR$^+$CD56$^+$ cells in skin repair (Driskell et al., 2013; Johnston et al., 2013; Paquet-Fifield et al., 2009; Parrinello et al., 2010) or neurilemmoma and neurofibroma formation (Ribeiro et al., 2013) is currently available, further research on these subjects is warranted.

EXPERIMENTAL PROCEDURES

Human Cell Isolation, Proliferation, and Characterization

Human adult foreskins were obtained from voluntary circumcisions of healthy donors (average 18.24 years of age, range 1–71 years; n = 74) with their informed consent and with protocol approval by the relevant IRB (CEIC Gipuzkoa). Human SKPs were derived as previously described (Toma et al., 2005), first by disaggregating dermal pieces onto unicellular suspensions through incubation in Type I collagenase (or Liberase DH) at 37°C, and then growing them as spheres in the presence of EGF and bFGF. For immunocytochemistry, cells were fixed in 4% paraformaldehyde and stained as previously described (Gago et al., 2009) using

Figure 4. In Situ Localization of p75NTR$^+$CD56$^+$ Cells in Human Dermis

(A) Dermal whole-mounts permit visualization of the subepidermal nerve and vascular plexus (Tschachler et al., 2004).

(B) Tissue whole-mount and immunofluorescence analyses showed p75NTR and CD56 double-positive fibers, as well as other fibrous structures expressing p75NTR only. Scale bar, 20 μm.

(C) Confocal 3D projections of p75NTR$^+$ cells show they sit at a perivascular location surrounding CD31$^+$ blood vessels. Scale bar, 20 μm.

(D) p75NTR$^+$CD56$^+$ peripheral nerves run parallel to blood vessels. Scale bar, 20 μm.

(E) Higher-magnification image shows a CD31$^+$ precapillary arteriole (white arrow) (Armulik et al., 2011) surrounded by p75NTR$^+$CD56$^-$ pericytes (red arrow) and p75NTR$^+$CD56$^+$ nerve fibers (green arrow). Scale bar, 10 μm.

(F–H) Whole mount immunolabeled with anti-p75NTR and anti-NG2 antibodies. Scale bar, 20 μm.

(I–L) Whole mount immunolabeled with anti-p75NTR and anti-SMA antibodies. Scale bar, 20 μm.

(M–P) Whole mount immunolabeled with anti-p75NTR and anti-PGP9.5 antibodies. Scale bar, 50 μm.

(Q–T) Whole mount immunolabeled with anti-p75NTR and anti-MAP2 antibodies, with the latter showing a punctate pattern (white arrowheads in T). Scale bar, 20 μm.

(U–X) Whole mount immunolabeled with anti-p75NTR and anti-Peripherin antibodies. Scale bar, 20 μm. In most sections, nuclei were counterstained with Hoechst 33258 (blue) as indicated.

See also Table S2 and Movies S3 and S4.

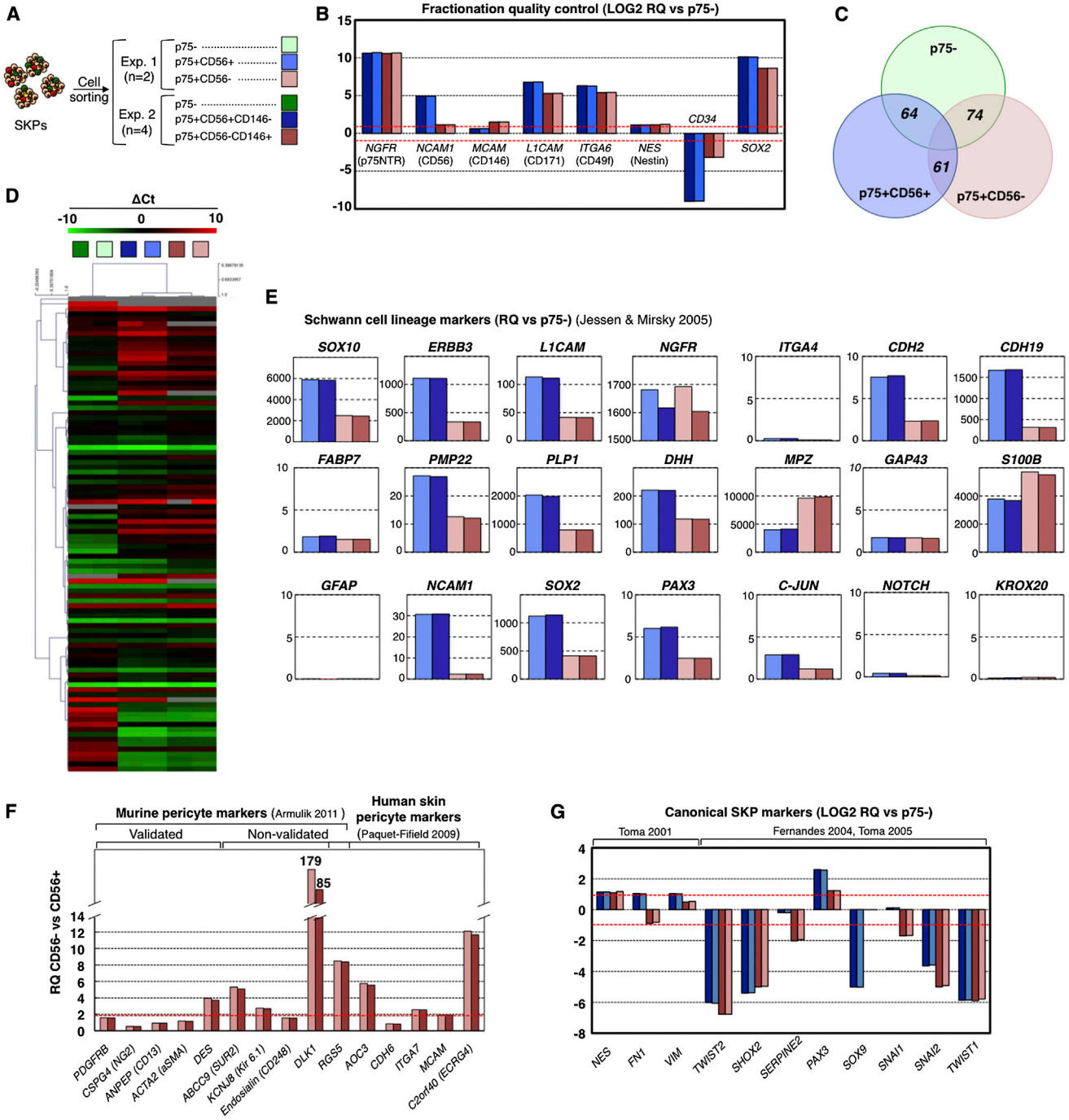

Figure 5. Gene-Expression Characterization of Human Dermis-Derived NPCs

(A) Cell sortings for p75NTR and CD56.

(B) Transcriptomic analyses of the sorted cell subpopulations, showing the specificity of the fractionation procedure. Log2 relative quantification (Log2 RQ) as compared with $p75NTR^{-}$ cells.

(C) Venn diagram showing differentially expressed genes (FC > 2) from qRT-PCR data.

(D) Hierarchical clustering (Pearson correlation) based on qRT-PCR data. Cell populations are color-coded as in (A).

(E) Expression of Schwann cell lineage markers in sorted cell fractions. RQ as compared with $p75NTR^{-}$ cells.

(F) Expression of pericyte lineage markers in $p75NTR^{+}CD56^{-}$ cell fractions. RQ as compared with double-positive cells.

(legend continued on next page)

the primary antibodies detailed in Table S2. Images were acquired on a LSM510 META confocal microscope (Zeiss) using the ZEN 2008 sp2 software package (v. 4.2). Adult human heart tissue was harvested from discarded pathological specimens at the time of heart transplantation under the supervision of the UW Institutional Review Board. Biopsies were stored in Ca^{2+}/Mg^{2+}-free Dulbecco's PBS (DPBS; Cellgro) supplemented with 2% penicillin/streptomycin (P/S) and processed no later than 4–6 hr postsurgery. Briefly, to obtain single cells, heart pieces were washed with DPBS, cut into small pieces (1–2 mm^3 pieces), and incubated in Type IV collagenase (1 mg/ml; GIBCO), Dispase (0.15 mg/ml; GIBCO), and DNase I (75 μg/ml; Sigma) as described above for 30–60 min at 37°C until partially digested. Tissues were manually dissociated by repeated pipetting until single cells were obtained. The cell suspension was centrifuged (5 min, 1,200 rpm) and the pellet was resuspended and passed through a 40 μm cell strainer (BD Biosciences). Then, 25,000 cells/cm^2 were cultured in T-75 culture flasks (BD Falcon) precoated with fibronectin (20 μg/ml DPBS) with growth media (IMDM with 20% FBS, 1% P/S, 1% L-glutamine, and 0.001% 2-mercaptoethanol). Floating cells and debris were eliminated after 24 hr and new medium was added. Heart-derived precursor cells with a fibroblast morphology were observed after 3 days in culture, and cardiospheres were derived as previously described (Gago-Lopez et al., 2014). In vitro differentiation was assessed as previously described (Gago et al., 2009).

Mouse Cell Isolation, Culture, and Differentiation

Animals were used in accordance with the relevant guidelines (European Directive 2010/63/EU, Spanish Law 6/2013 and Royal Decree 53/2013) and the protocol was approved by the Biodonostia Animal Care Committee. Murine SKPs were obtained from dorsal skin samples from adult *SOX2*^{EGFP} mice (n = 6; kindly provided by Konrad Hochedlinger, Harvard University). Animals (6–8 months old) were sacrificed by CO_2 inhalation and the back skin was carefully dissected free of other tissue, cut into 2–3 mm^3 pieces, washed two times in Hank's balanced salt solution (HBSS; GIBCO), and digested with 1 mg/ml collagenase XI (Sigma) for 1 hr at 37°C. The tissue pieces were resuspended in Dulbecco's modified Eagle's medium (DMEM)/F12 3:1 with 1% P/S (GIBCO) and mechanically dissociated by vigorous pipetting. The suspension was filtered through a 40 μm cell strainer (BD Biosciences), centrifuged at 1,500 rpm for 5 min, and resuspended in proliferation medium. Cells were cultured at a density of 300,000 cells/ml in untreated dishes. Further passages were done as described above for human SKP dermospheres. Dermospheres at day 7 or 14 were used for sorting experiments. Neural stem cells (NSCs) were isolated from *SOX2*^{EGFP} mice SVZ (n = 5, 6–8 weeks old) as previously described (Doetsch et al., 1999). Brains were placed into NSC basal medium (DMEM/F12 1:1, supplemented with 1% N2, 2% B27, 0.6% [w/v] glucose and P/S [GIBCO]). Coronal sections were cut and SVZ tissue was dissected out and digested for 20 min at 37°C with 1 mg/ml papain (Roche) (previously activated at 37°C for 30 min), and 0.25 mg/ml DNase I dissolved in NSC basal medium. Cells were dissociated by gentle pipetting and a 10× volume of NSC basal medium was added to end the digestion. The cell suspension was centrifuged for 5 min at 1,000 rpm and filtered through 40 μm cell strainers (BD Biosciences). The cells were then plated in uncoated six-well plates in NSC proliferating medium (NSC basal medium plus 40 ng/ml bFGF [GIBCO] and 20 ng/ml EGF [BD Biosciences]). Neurospheres were passaged after 10 days of culture by harvesting them by centrifugation (1,000 rpm for 5 min) and dissociated with Accutase solution (Invitrogen). Neurospheres of passage 2 were plated onto 12-mm-diameter coverslips that were previously treated to improve adherence to extracellular matrix from 804G cells (Gago et al., 2009), cultured in attachment for 3 weeks, and then differentiated in Schwann medium for another 10 days.

Flow Cytometry

Cells were stained with the following antibodies (BD Biosciences): anti-CD271 (clone C40-1457, conjugated to PE or APC), anti-CD56 Alexa 647 (clone B159), anti-CD56 FITC (clone NCAM 16.2), anti-CD34 PE (clone 8G12), and anti-CD146 PECy7 (clone P1H12). To control for nonspecifically bound fluorescence, the isotype antibodies used (BD Biosciences) were clones MOPC-31C (PE) and MOPC-21 (PECy7, APC and Alexa 647). Data were acquired on FACSCalibur or FACSCanto A flow cytometers (BD Biosciences). The instrument's performance was evaluated with the use of calibrite beads or CST beads, respectively. Scatter and fluorescence parameters were acquired in linear and logarithmic modes, respectively, and detected by the following bandpass filters: 530/30 (Sytox Green viability dye; Invitrogen), 585/42 (PE), 660/20 (Alexa 647; APC), and 780/60 (PECy7). FACSDiva or CellQuest-Pro software (BD Biosciences) was used for data acquisition, and FACSDiva or FlowJo (Verity) software was used for analyses. The pulse area (FACSCanto A) or height (FACSCalibur) was used in all analyzed parameters.

Cell Sorting

Cell-sorting experiments were done on a FACSAria III cell sorter (BD Biosciences) at low sheath pressure with a 100 μm nozzle. Scatter and fluorescence parameters were acquired in linear and log modes, respectively. Photomultiplier (PMT) settings were established on live (Sytox Green negative) singlets by using unstained cells. Nonspecific binding was evaluated with the corresponding isotypic controls used at the same concentration as the antibody of interest.

In Ovo Cell Transplantation

Chicken eggs were incubated until they reached HH17. An incision was made into the anterior medial corner of the somite in the lumbar region. Human skin-derived p75NTR$^+$, p75 NTR$^-$, or unsorted cells (30,000 cells ml^{-1}) were transplanted as previously described

(G) Expression of SKP markers in sorted cell fractions. Log2 relative quantification (Log2 RQ) as compared with p75NTR$^-$ cells. The red lines demarcate the relative quantification level difference that is considered significant, i.e., where the FC between fractions equals ± 2 (± one Log2 in B and G, and RQ = 2 in F).
See also Figures S3 and S4 and Table S1.

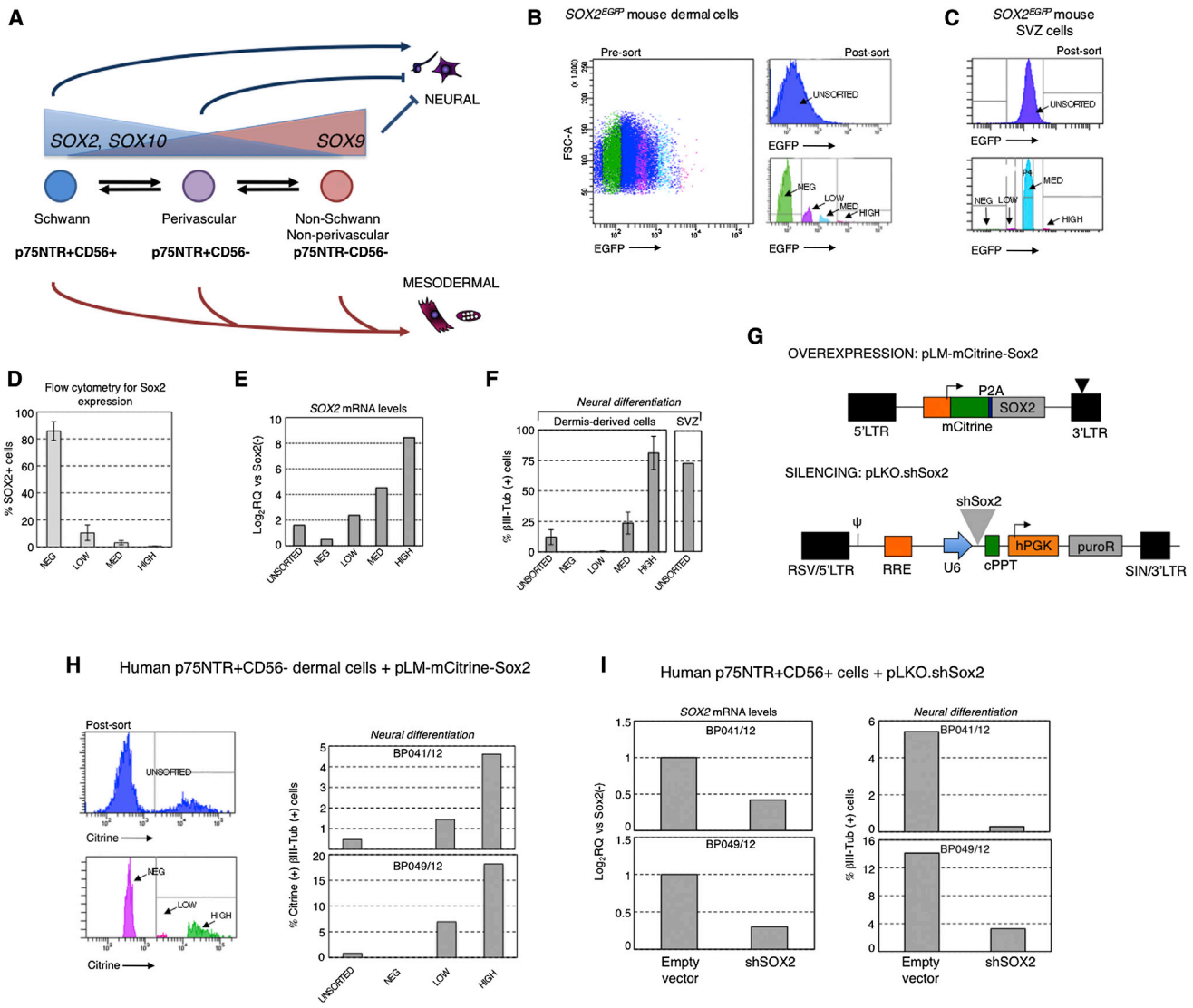

Figure 6. *SOX2* Expression Levels Regulate the Neural Competence of Dermis-Derived Precursors

(A) "Cellular states" model. Interstitial precursors, such as those isolated from the dermis, might be detected as "Schwann," "perivascular," or "non-Schwann, nonperivascular" states. These cellular states might be functionally interchangeable through cell intrinsic or context-dependent modulation of *SOX2*, *SOX10*, and *SOX9* gene-expression levels as depicted. Although the three precursor cell states generate mesodermal progeny, only p75NTR^{+}CD56^{+} (*SOX2*^{hi}) cells retain neural competence.

(B) In *SOX2*^{EGFP} mice, dermis-derived cells were sorted into negative (NEG), low (LOW), medium (MED), and high (HIGH) subpopulations according to their EGFP levels.

(C) NSCs of the SVZ of *SOX2*^{EGFP} mice were mostly found in the EGFP medium (MED) fraction.

(D) SOX2 levels correlated with EGFP in the dermis-derived fractions, as shown by flow cytometry (n = 4). Error bars indicate SD.

(E) Endogenous *SOX2* mRNA levels correlated with EGFP in the dermis-derived fractions (n = 2).

(F) The neural competence of the murine dermal cell subpopulations (left panel, n = 3) correlated with higher *SOX2* levels. Unsorted SVZ cells (right panel, n = 2) differentiated to levels similar to those observed for the dermis-derived EGFP^{hi} fraction. Error bars indicate SD.

(G) Lentiviral constructs used for the gain- and loss-of-function experiments, which were done by stable overexpression and silencing of *SOX2*.

(H) Overexpression of *SOX2*-mCitrine in p75NTR^{+}CD56^{-} cells and sorting of the mCitrine NEG, LOW, and HIGH cell fractions resulted in correlative neural competence as determined by βIII Tubulin cell counts in differentiation culture. Each panel represents an independent biopsy (n = 2).

(legend continued on next page)

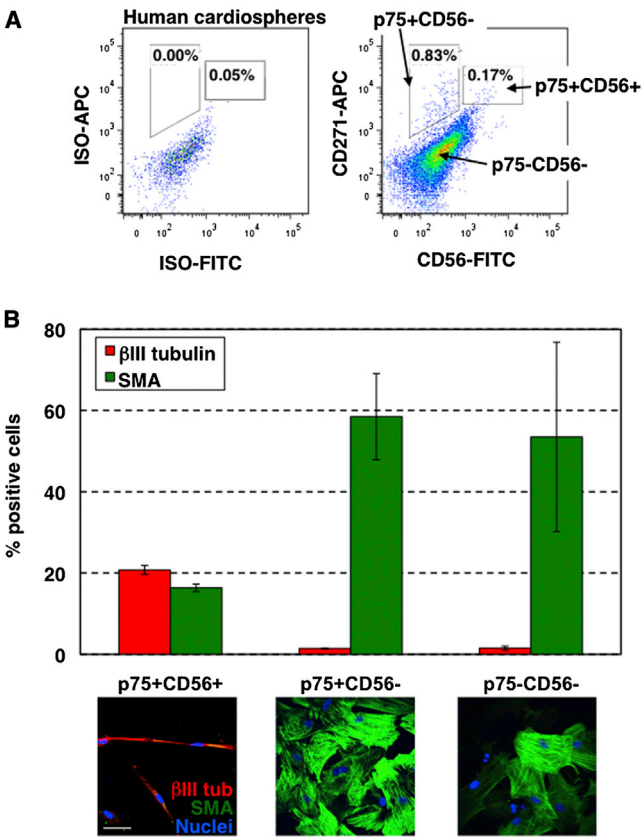

Figure 7. Human Cardiosphere-Derived p75NTR$^+$CD56$^+$ Cells Present NPC Properties

(A) Human cardiosphere-derived cell isolation strategy. Double-positive cells constituted a minor fraction (0.17%, n = 2) of heart-derived precursor cells.

(B) In vitro differentiation of p75NTR$^+$CD56$^+$, p75NTR$^+$CD56$^-$, and p75NTR-CD56$^-$ cell fractions sorted from human cardiospheres, and quantification of neural (βIII tubulin$^+$) and mesodermal (SMA$^+$) progeny (n = 2). Scale bar, 10 μm. Error bars indicate SD.

(Fernandes et al., 2004). Embryos were incubated for 56 hr (until HH26), sacrificed, and analyzed by immunohistochemistry. Sections (30 μm thick) were cut on a MA752 (Campden Instruments) or VT1000S (Leica) vibroslicer and analyzed by confocal microscopy on a Leica TCS SP5 microscope.

Cell-Surface Marker Screening

A total of 242 primary antibodies (Lyoplate, BD Biosciences) were stained with Alexa 647-conjugated secondary antibodies and costained with anti-CD271 PE (clone C40-1457). Data were confirmed by serial repetition of positives and controlled by known negative antibodies. Population boundary limits were based on (1) cells only for evaluation of autofluorescence and setting of PMTs, (2) isotypic control for anti-CD271 (same isotype, concentration, and fluorochrome), (3) secondary antibody only (rat anti-mouse IgG or goat anti-rat IgG Alexa 647), (4) FMO to set boundaries and check compensation for CD271, and (5) anti-CD271 plus secondary antibody to ascertain any nonspecific Alexa 647 background on p75NTR$^+$ cells. A marker was considered "positive" when expressed by at least 35% of the cells and "upregulated" when the fold change (FC) was ≥2.

RNA Extraction and Real-Time PCR

Total RNA was extracted from sorted cell pellets obtained from pooled biopsies using the miRNeasy mini kit and QIAcube workstation (QIAGEN). Gene expression was analyzed in 96-well plates with predispensed TaqMan probes (Life Technologies). RNAs (75 ng) were preamplified (14 cycles) using the TaqMan PreAmp Master Mix Kit (Life Technologies), PCR amplified, and measured on a StepOne Real-Time PCR System (Life Technologies). DataAssist (Life Technologies), Excel (Microsoft), and MeV (Saeed et al., 2006) software suites were used for analyses and quality control of the data. After the expression of endogenous control mRNAs was assessed, the median expression of all 95 genes was used to normalize (by discrete cosine transform [DCT]) the data due to its lower variability. Relative quantification (RQ; 2^{-DDCT}) analyses were performed for each comparison and the significance threshold was set at an FC of 2.

Lentiviral Construct-Mediated Overexpression and Silencing of *SOX2*

For stable overexpression of *SOX2*, lentiviral transduction was performed with a pLM-mCitrine-Sox2 construct (Addgene plasmid 23242) (Papapetrou et al., 2009) and pCMV-GFP as control. After incubation with polybrene (H9268-56; Sigma), cells were infected at a multiplicity of infection of 10 for 6 hr, and then medium without serum was changed to proliferation medium. Expanded cells were sorted based on SOX2-mCitrine expression levels. For *SOX2* silencing, cells were infected with pLKO.shSox2 (TRCN0000003253; Sigma) and control pLKO.1 lentiviral vectors. Infected cells were selected and expanded in attachment in the presence of 2 μg/ml puromycin and then maintained with 0.2 μg/ml puromycin (P9620; Sigma). For qRT-PCR, total RNA was extracted and RNAs were preamplified as above. Gene expression was analyzed in 384-well plates using TaqMan probes (Life Technologies). The mRNA level was measured on a 7900HT Real-Time PCR System (Life Technologies). The Excel software suite (Microsoft) was used for analyses and quality control of the data. The expression of endogenous control mRNAs (both TBP and GAPDH) was used to normalize (by DCT) the data due to its lower variability. RQ (2^{-DDCT}) analyses were performed for each comparison and the significance threshold was set at an FC of 2.

(I) Silencing of *SOX2* by lentiviral expression of shSox2 in p75NTR$^+$CD56$^+$ cells and selective expansion of transduced cells resulted in a concomitant reduction in the neural differentiation capacity of transduced cells. Each panel represents an independent biopsy (n = 2).

See also Figure S5.

In Vitro Myelinization Assays

Pregnant Sprague-Dawley rats (Charles River Laboratories) were sacrificed by CO_2 inhalation and E14 embryos were immediately removed by caesarean section and placed onto Petri dishes with HBSS to isolate the spinal cord and DRG. Cells predifferentiated in Schwann cell medium were cocultured with the rat explants in CoM2 medium (Chen et al., 2010) or CoM2 supplemented with nerve growth factor and ascorbic acid (Biernaskie et al., 2009). The media were refreshed every 2–3 days and cocultures were analyzed by immunofluorescence 1 and 2 weeks after explant addition.

Statistical Analyses

Kolmogorov-Smirnov tests were used to generate p values for comparison of expression distributions. For multiple group comparisons, one-way ANOVAs were performed. The number of biological replicates (n) for each experiment and average ± SD are indicated when applicable, and $p < 0.05$ was considered statistically significant (*).

SUPPLEMENTAL INFORMATION

Supplemental Information includes five figures, two tables, and four movies and can be found with this article online at http://dx.doi.org/10.1016/j.stemcr.2014.09.009.

AUTHOR CONTRIBUTIONS

U.E. and A.P.-S.V. performed most of the experimental research. N.G.-L. had the original idea for the study, started the project in A.I.'s lab, and contributed heart-tissue data from the lab of R.M.L. M.G.-D. performed in ovo experiments. A.A. and M.P.L.-M. obtained flow-cytometry data. V.P.-L., H.I., and I.B. provided technical support. H.I., M.M.-C., and D.O. performed expression analyses. A.V.-I. performed in vitro myelinization experiments. O.L., A.M., and A.G.M. provided viral constructs and helped conduct loss- and gain-of-function experiments. A.I. directed all research, raised funds, and wrote the manuscript.

ACKNOWLEDGMENTS

We are thankful to Drs. I. Eizaguirre, J.P. Sanz-Jaka, and J.J. Poza for providing healthy donor tissue samples; K. Hochedlinger for providing *SOX2*^{EGFP} mice; and L. Reichardt for the anti-GalC antibody. We are also indebted to F.D. Miller for sharing unpublished data and support. T. Aragón, M. Arrasate, H. Etchevers, A. López de Munain, R. Paus, and R. Sánchez-Pernaute provided helpful experimental suggestions and comments on the manuscript. This work was financed by grants provided by Ministerio de Economía y Competitividad (Instituto de Salud Carlos III [PI13/02172; PI10/02871] and INNPACTO [IPT-300000-2010-17] programs), Diputación Foral de Gipuzkoa (OF 30/2014, OF 98/2012, 53/2011, and 94/2008), the European Union (Poctefa-Interreg-IV-A; Refbio13/Biod/009), and Gobierno Vasco (Saio12-PE12BN010; Saio10-PE10BF01). A.P.-S.V., U.E., and H.I. received studentships from the Department of Education, University and Research of the Basque Government (BFI08-150, BFI10-262, and PRE2013-1-1068, respectively). A.I. was supported by the "Programa I3SNS" (CES09/015) from Instituto de Salud Carlos III and by Osakidetza (Spain).

Received: May 11, 2013
Revised: September 10, 2014
Accepted: September 11, 2014
Published: October 16, 2014

REFERENCES

Adly, M.A., Assaf, H.A., and Hussein, M.R. (2009). Expression pattern of p75 neurotrophin receptor protein in human scalp skin and hair follicles: hair cycle-dependent expression. J. Am. Acad. Dermatol. *60*, 99–109.

Armulik, A., Genové, G., and Betsholtz, C. (2011). Pericytes: developmental, physiological, and pathological perspectives, problems, and promises. Dev. Cell *21*, 193–215.

Bergsland, M., Ramsköld, D., Zaouter, C., Klum, S., Sandberg, R., and Muhr, J. (2011). Sequentially acting Sox transcription factors in neural lineage development. Genes Dev. *25*, 2453–2464.

Biernaskie, J., Paris, M., Morozova, O., Fagan, B.M., Marra, M., Pevny, L., and Miller, F.D. (2009). SKPs derive from hair follicle precursors and exhibit properties of adult dermal stem cells. Cell Stem Cell *5*, 610–623.

Chen, Z., Ma, Z., Wang, Y., Li, Y., Lü, H., Fu, S., Hang, Q., and Lu, P.H. (2010). Oligodendrocyte-spinal cord explant co-culture: an in vitro model for the study of myelination. Brain Res. *1309*, 9–18.

Cheng, L., Huang, Z., Zhou, W., Wu, Q., Donnola, S., Liu, J.K., Fang, X., Sloan, A.E., Mao, Y., Lathia, J.D., et al. (2013). Glioblastoma stem cells generate vascular pericytes to support vessel function and tumor growth. Cell *153*, 139–152.

Doetsch, F., Caillé, I., Lim, D.A., García-Verdugo, J.M., and Alvarez-Buylla, A. (1999). Subventricular zone astrocytes are neural stem cells in the adult mammalian brain. Cell *97*, 703–716.

Driskell, R.R., Giangreco, A., Jensen, K.B., Mulder, K.W., and Watt, F.M. (2009). Sox2-positive dermal papilla cells specify hair follicle type in mammalian epidermis. Development *136*, 2815–2823.

Driskell, R.R., Lichtenberger, B.M., Hoste, E., Kretzschmar, K., Simons, B.D., Charalambous, M., Ferron, S.R., Herault, Y., Pavlovic, G., Ferguson-Smith, A.C., and Watt, F.M. (2013). Distinct fibroblast lineages determine dermal architecture in skin development and repair. Nature *504*, 277–281.

Dupin, E., and Sommer, L. (2012). Neural crest progenitors and stem cells: from early development to adulthood. Dev. Biol. *366*, 83–95.

Ellis, P., Fagan, B.M., Magness, S.T., Hutton, S., Taranova, O., Hayashi, S., McMahon, A., Rao, M., and Pevny, L. (2004). SOX2, a persistent marker for multipotential neural stem cells derived from embryonic stem cells, the embryo or the adult. Dev. Neurosci. *26*, 148–165.

Fauquier, T., Rizzoti, K., Dattani, M., Lovell-Badge, R., and Robinson, I.C. (2008). SOX2-expressing progenitor cells generate all of the major cell types in the adult mouse pituitary gland. Proc. Natl. Acad. Sci. USA *105*, 2907–2912.

Fernandes, K.J., McKenzie, I.A., Mill, P., Smith, K.M., Akhavan, M., Barnabé-Heider, F., Biernaskie, J., Junek, A., Kobayashi, N.R., Toma, J.G., et al. (2004). A dermal niche for multipotent adult skin-derived precursor cells. Nat. Cell Biol. *6*, 1082–1093.

Gago, N., Pérez-López, V., Sanz-Jaka, J.P., Cormenzana, P., Eizaguirre, I., Bernad, A., and Izeta, A. (2009). Age-dependent depletion of human skin-derived progenitor cells. Stem Cells *27*, 1164–1172.

Gago-Lopez, N., Awaji, O., Zhang, Y., Ko, C., Nsair, A., Liem, D., Stempien-Otero, A., and MacLellan, W.R. (2014). THY-1 receptor expression differentiates cardiosphere-derived cells with divergent cardiogenic differentiation potential. Stem Cell Rep. *2*, 576–591.

Hill, R.P., Gledhill, K., Gardner, A., Higgins, C.A., Crawford, H., Lawrence, C., Hutchison, C.J., Owens, W.A., Kara, B., James, S.E., and Jahoda, C.A. (2012). Generation and characterization of multipotent stem cells from established dermal cultures. PLoS ONE *7*, e50742.

Hunt, D.P., Jahoda, C., and Chandran, S. (2009). Multipotent skin-derived precursors: from biology to clinical translation. Curr. Opin. Biotechnol. *20*, 522–530.

Hutton, S.R., and Pevny, L.H. (2011). SOX2 expression levels distinguish between neural progenitor populations of the developing dorsal telencephalon. Dev. Biol. *352*, 40–47.

Jessen, K.R., and Mirsky, R. (2005). The origin and development of glial cells in peripheral nerves. Nat. Rev. Neurosci. *6*, 671–682.

Jessen, K.R., and Mirsky, R. (2008). Negative regulation of myelination: relevance for development, injury, and demyelinating disease. Glia *56*, 1552–1565.

Jinno, H., Morozova, O., Jones, K.L., Biernaskie, J.A., Paris, M., Hosokawa, R., Rudnicki, M.A., Chai, Y., Rossi, F., Marra, M.A., and Miller, F.D. (2010). Convergent genesis of an adult neural crest-like dermal stem cell from distinct developmental origins. Stem Cells *28*, 2027–2040.

Johnston, A.P., Naska, S., Jones, K., Jinno, H., Kaplan, D.R., and Miller, F.D. (2013). Sox2-mediated regulation of adult neural crest precursors and skin repair. Stem Cell Rep. *1*, 38–45.

Joseph, N.M., and Morrison, S.J. (2005). Toward an understanding of the physiological function of Mammalian stem cells. Dev. Cell *9*, 173–183.

Kaidoh, T., and Inoué, T. (2008). N-cadherin expression in palisade nerve endings of rat vellus hairs. J. Comp. Neurol. *506*, 525–534.

Karow, M., Sánchez, R., Schichor, C., Masserdotti, G., Ortega, F., Heinrich, C., Gascón, S., Khan, M.A., Lie, D.C., Dellavalle, A., et al. (2012). Reprogramming of pericyte-derived cells of the adult human brain into induced neuronal cells. Cell Stem Cell *11*, 471–476.

Kaucká, M., and Adameyko, I. (2014). Non-canonical functions of the peripheral nerve. Exp. Cell Res. *321*, 17–24.

Kim, J., Lo, L., Dormand, E., and Anderson, D.J. (2003). SOX10 maintains multipotency and inhibits neuronal differentiation of neural crest stem cells. Neuron *38*, 17–31.

Krause, M.P., Dworski, S., Feinberg, K., Jones, K., Johnston, A.P.W., Paul, S., Paris, M., Peles, E., Bagli, D., Forrest, C.R., et al. (2014). Direct genesis of functional rodent and human Schwann cells from skin mesenchymal precursors. Stem Cell Rep. *3*, 85–100.

Kruger, G.M., Mosher, J.T., Bixby, S., Joseph, N., Iwashita, T., and Morrison, S.J. (2002). Neural crest stem cells persist in the adult gut but undergo changes in self-renewal, neuronal subtype potential, and factor responsiveness. Neuron *35*, 657–669.

Lemke, G., and Chao, M. (1988). Axons regulate Schwann cell expression of the major myelin and NGF receptor genes. Development *102*, 499–504.

Liu, S., Liu, S., Wang, X., Zhou, J., Cao, Y., Wang, F., and Duan, E. (2011). The PI3K-Akt pathway inhibits senescence and promotes self-renewal of human skin-derived precursors in vitro. Aging Cell *10*, 661–674.

Locher, H., de Rooij, K.E., de Groot, J.C., van Doorn, R., Gruis, N.A., Lowik, C.W., Chuva de Sousa Lopes, S.M., Frijns, J.H., and Huisman, M.A. (2013). Class III beta-tubulin, a novel biomarker in the human melanocyte lineage. Differentiation *85*, 173–181.

Mirsky, R., Jessen, K.R., Brennan, A., Parkinson, D., Dong, Z., Meier, C., Parmantier, E., and Lawson, D. (2002). Schwann cells as regulators of nerve development. J. Physiol. Paris *96*, 17–24.

Morrison, S.J., White, P.M., Zock, C., and Anderson, D.J. (1999). Prospective identification, isolation by flow cytometry, and in vivo self-renewal of multipotent mammalian neural crest stem cells. Cell *96*, 737–749.

Papapetrou, E.P., Tomishima, M.J., Chambers, S.M., Mica, Y., Reed, E., Menon, J., Tabar, V., Mo, Q., Studer, L., and Sadelain, M. (2009). Stoichiometric and temporal requirements of Oct4, Sox2, Klf4, and c-Myc expression for efficient human iPSC induction and differentiation. Proc. Natl. Acad. Sci. USA *106*, 12759–12764.

Paquet-Fifield, S., Schlüter, H., Li, A., Aitken, T., Gangatirkar, P., Blashki, D., Koelmeyer, R., Pouliot, N., Palatsides, M., Ellis, S., et al. (2009). A role for pericytes as microenvironmental regulators of human skin tissue regeneration. J. Clin. Invest. *119*, 2795–2806.

Parrinello, S., Napoli, I., Ribeiro, S., Wingfield Digby, P., Fedorova, M., Parkinson, D.B., Doddrell, R.D., Nakayama, M., Adams, R.H., and Lloyd, A.C. (2010). EphB signaling directs peripheral nerve regeneration through Sox2-dependent Schwann cell sorting. Cell *143*, 145–155.

Ranscht, B., Clapshaw, P.A., Price, J., Noble, M., and Seifert, W. (1982). Development of oligodendrocytes and Schwann cells studied with a monoclonal antibody against galactocerebroside. Proc. Natl. Acad. Sci. USA *79*, 2709–2713.

Reinisch, C.M., and Tschachler, E. (2012). The dimensions and characteristics of the subepidermal nerve plexus in human skin—terminal Schwann cells constitute a substantial cell population within the superficial dermis. J. Dermatol. Sci. *65*, 162–169.

Ribeiro, S., Napoli, I., White, I.J., Parrinello, S., Flanagan, A.M., Suter, U., Parada, L.F., and Lloyd, A.C. (2013). Injury signals cooperate with Nf1 loss to relieve the tumor-suppressive environment of adult peripheral nerve. Cell Rep. *5*, 126–136.

Saeed, A.I., Bhagabati, N.K., Braisted, J.C., Liang, W., Sharov, V., Howe, E.A., Li, J., Thiagarajan, M., White, J.A., and Quackenbush, J. (2006). TM4 microarray software suite. Methods Enzymol. *411*, 134–193.

Takahashi, M., and Osumi, N. (2005). Identification of a novel type II classical cadherin: rat cadherin19 is expressed in the cranial ganglia and Schwann cell precursors during development. Dev. Dyn. *232*, 200–208.

Taranova, O.V., Magness, S.T., Fagan, B.M., Wu, Y., Surzenko, N., Hutton, S.R., and Pevny, L.H. (2006). SOX2 is a dose-dependent

regulator of retinal neural progenitor competence. Genes Dev. *20*, 1187–1202.

Toma, J.G., Akhavan, M., Fernandes, K.J., Barnabé-Heider, F., Sadikot, A., Kaplan, D.R., and Miller, F.D. (2001). Isolation of multipotent adult stem cells from the dermis of mammalian skin. Nat. Cell Biol. *3*, 778–784.

Toma, J.G., McKenzie, I.A., Bagli, D., and Miller, F.D. (2005). Isolation and characterization of multipotent skin-derived precursors from human skin. Stem Cells *23*, 727–737.

Tschachler, E., Reinisch, C.M., Mayer, C., Paiha, K., Lassmann, H., and Weninger, W. (2004). Sheet preparations expose the dermal nerve plexus of human skin and render the dermal nerve end organ accessible to extensive analysis. J. Invest. Dermatol. *122*, 177–182.

Wang, X., Liu, S., Zhao, Q., Li, N., Zhang, H., Zhang, X., Lei, X., Zhao, H., Deng, Z., Qiao, J., et al. (2014). Three-dimensional hydrogel scaffolds facilitate in vitro self-renewal of human skin-derived precursors. Acta Biomater. *10*, 3177–3187.

Wanjare, M., Kusuma, S., and Gerecht, S. (2014). Defining differences among perivascular cells derived from human pluripotent stem cells. Stem Cell Rep. *2*, 561–575.

Wanner, I.B., Guerra, N.K., Mahoney, J., Kumar, A., Wood, P.M., Mirsky, R., and Jessen, K.R. (2006). Role of N-cadherin in Schwann cell precursors of growing nerves. Glia *54*, 439–459.

Wegner, M. (2011). SOX after SOX: SOXession regulates neurogenesis. Genes Dev. *25*, 2423–2428.

Wong, C.E., Paratore, C., Dours-Zimmermann, M.T., Rochat, A., Pietri, T., Suter, U., Zimmermann, D.R., Dufour, S., Thiery, J.P., Meijer, D., et al. (2006). Neural crest-derived cells with stem cell features can be traced back to multiple lineages in the adult skin. J. Cell Biol. *175*, 1005–1015.